Longitudinal injection scheme using short pulse kicker for small aperture electron storage rings

M. Aiba,* M. Böge, F. Marcellini, Á. Saá Hernández, and A. Streun

Paul Scherrer Institut, CH-5232 Villigen PSI, Switzerland

(Received 20 August 2014; published 20 February 2015)

Future light sources aim at achieving a diffraction limited photon beam both in the horizontal and vertical planes. High gradient quadrupoles and strong chromaticity correction sextupoles in a corresponding ultra-low emittance ring may restrict the physical and dynamic aperture of the storage ring such that off-axis injection and accumulation may become impossible. We propose a longitudinal injection scheme, i.e., injecting an electron bunch onto the closed orbit with a time offset with respect to the circulating bunches. The temporal separation enables a pulsed dipole kicker to situate the injected bunch transversely on-axis without disturbing the circulating bunches if the pulse length is shorter than the bunch spacing. The injected bunch is finally merged to a circulating bunch through synchrotron radiation damping. We present the scheme in detail and its application to the lattice of the MAX IV 3 GeV storage ring. The requirements and feasibility of the pulsed dipole kicker are also discussed.

DOI: 10.1103/PhysRevSTAB.18.020701 PACS numbers: 29.20.db, 29.27.Ac

I. INTRODUCTION

The performance of light sources has been progressively approaching one of its ultimate goals, i.e., achieving a double plane diffraction limited photon beam. The fundamental approach for this is lowering the transverse electron beam emittance both in the horizontal and vertical planes to the picometer regime. A storage ring realizing such ultra-low emittances is normally composed of quadrupoles with rather high gradient, and thus the available physical aperture decreases. In addition the dynamic aperture may become small because of strong sextupoles which are necessary to compensate for the chromatic effects arising from these strong quadrupoles.

At the same time, one of the most important features in light sources is the high stability of the photon beam. The so-called *top-up injection* [1,2] is incorporated into most third generation light sources, where a frequent beam injection on top of the circulating bunches is carried out to keep the electron beam current essentially constant. The relative current fluctuation is within a small range (dead-band), which is typically a few 10^{-3} [2]. Our primary goal is therefore to establish an on-axis injection scheme which is fully transparent to the circulating bunches.

According to Liouville's theorem, a bunch cannot be injected to the same phase-space volume occupied by the circulating bunches at the time of injection although it will later be merged into a circulating bunch because of synchrotron radiation damping. We review the existing injection schemes keeping this rule in mind.

The conventional injection scheme into electron storage rings employs a static septum and a kicker bump (see, e.g., [3]). The latter rises to bring the closed orbit to the vicinity of the septum at the time of injection and falls within one electron beam revolution or a few to prevent the injected bunch being lost at the septum. In the conventional scheme, the injected bunch is transversely separate from the circulating bunches, and thus it is referred to as off-axis injection. It requires a relatively large physical and dynamic aperture of the ring to capture the injected beam because the transverse separation must be larger than the septum thickness.

It is noted that, though this scheme is in principle transparent to the circulating bunches, the kicker bump unfortunately introduces adverse disturbance to the photon beam even when intensive efforts are made to close the orbit bump. Another important goal is therefore to avoid such a kicker bump.

An injection scheme utilizing *multipole kicker* and avoiding the inclusion of a kicker bump has been proposed and experimentally examined [4]. The injected bunch passes through a pulsed multipole magnet with an offset from its center while the circulating bunches pass through the center. Therefore, the disturbance to the circulating bunches is significantly suppressed. The scheme is compatible with top-up injection. Nevertheless, it is an off-axis injection scheme that requires sufficient physical and dynamic aperture.

An on-axis, "swap-out" injection scheme that is suitable for reduced-aperture machines has been proposed [5]. With this scheme, circulating bunches are completely replaced, either bunch by bunch or with bunch trains, when beam

*masamitsu.aiba@psi.ch

current decreases below a top-up injection threshold. Swap-out injection, however, entails some disadvantages as discussed later.

In this paper we present another transparent injection scheme for reduced-aperture machines—longitudinal injection—where the injected bunch is longitudinally separate from the circulating bunches, i.e., injected with a time offset. The bunch can be injected transversely on-axis using a pulsed dipole kicker because the separation is realized in the longitudinal phase space. The circulating bunches are not disturbed if the kicker pulse length is shorter than the bunch spacing.

Two injection schemes, in which the longitudinal phase space was utilized for separation, have already been realized in lepton rings. In LEP, *synchrotron phase space injection* [6] was applied to realize an on-axis injection. The kicker bump was situated at a dispersive section. The bunches were injected with an energy offset and the injection orbit was matched to the off-momentum closed orbit. Another scheme was employed at VEPP-3. First, an rf system of ~8 MHz was used to realize a relatively long rf bucket at the injection energy. The bunches were injected with a time offset, damped with the synchrotron radiation and accumulated. Second, an rf system of ~72 MHz was turned on when the beam was accelerated to and/or kept at high energy [7]. The injection scheme that we present is also based on the separation in the longitudinal phase space but adapted to modern light sources: it requires neither a kicker bump nor a multiple rf system.

Our scheme is described in Sec. II, and an application to the lattice of the MAX IV 3 GeV storage ring is presented in Sec. III. The requirements and feasibility of the pulsed dipole kicker, which is a key component in the longitudinal injection scheme, are discussed in Sec. IV. The longitudinal injection scheme is further discussed in detail in Sec. V. Finally the conclusions are drawn in Sec. VI.

II. LONGITUDINAL INJECTION SCHEME

We first discuss the longitudinal particle motion in a storage ring taking into account the energy loss arising from synchrotron radiation. The motion can be described with the following equations of motion, assuming a relativistic beam:

$$\frac{dz}{dt} = -c\alpha\delta, \tag{1}$$

and

$$\frac{d\delta}{dt} = \frac{eV - U}{E_0 T_0}, \tag{2}$$

where z is the longitudinal coordinate with respect to the reference synchronous particle, c is the speed of light, α is the momentum compaction factor of the storage ring, δ is the relative momentum deviation, e is the electron charge, E_0 is the nominal beam energy, T_0 is the revolution period, and U is the energy loss per turn due to synchrotron radiation. V is the rf voltage, which is represented as

$$V(z) = V_0 \sin\left(2\pi f_{\mathrm{rf}} \frac{z}{c} + \psi_s\right), \tag{3}$$

where ψ_s is the synchronous phase.

The rf frequency, f_{rf}, is normally a high multiple of the revolution frequency, f_0, that is,

$$f_{\mathrm{rf}} = h f_0, \tag{4}$$

where h is the so-called harmonic number. The energy loss per turn depends on the momentum deviation and is approximately represented as

$$U(\delta) = U_0(1+\delta)^3, \tag{5}$$

for storage rings with transverse gradient-free bending magnets. U_0 is the energy loss per turn for the nominal beam energy. It is noted that the relative momentum deviation is approximated by the relative energy deviation for relativistic beams in these equations.

The operation point of electron storage rings is normally above transition, and α is positive. The synchronous phase is lower than 180 degrees because of the synchrotron radiation loss. The reference particle with the nominal momentum of the ring is considered to stay at the synchronous phase, where the synchrotron radiation loss equals the energy gain from the rf field.

The energy dependence of the radiation loss is the origin of radiation damping. If we assume that the energy loss is constant with the momentum deviation, the "static" rf bucket can be defined similarly to the moving (or accelerating) bucket. The synchronous phase, the bucket height, δ_B, and the synchrotron tune, Q_s, are given by

$$\psi_s = \pi - \arcsin\left(\frac{U_0}{V_0}\right), \tag{6}$$

$$\delta_B = \sqrt{-\frac{2eV_0}{\pi E_0 h\alpha}\left[\cos\psi_s + \left(\psi_s - \frac{\pi}{2}\right)\sin\psi_s\right]}, \tag{7}$$

and

$$Q_s = \sqrt{-\frac{h\alpha e V_0}{2\pi E_0}\cos\psi_s}. \tag{8}$$

See, e.g., [8] for the derivation of these equations.

From these equations, it is found that the longitudinal motion is parametrized with $h\alpha$, U_0/E_0 and V_0/E_0, i.e., the motion is uniquely determined when these three parameters

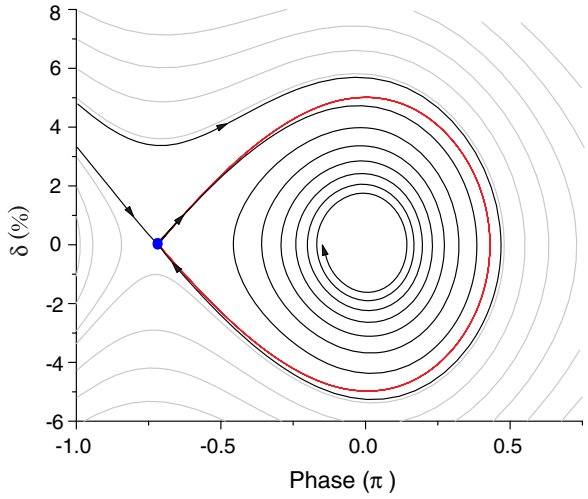

FIG. 1. Longitudinal phase space topologies with synchrotron radiation loss. The origin of the horizontal axis is shifted, corresponding to the synchronous phase. This example is for the synchronous phase of 2.71 rad (155 deg) and the bucket height of 5% according to Eq. (7). The black lines indicate the longitudinal acceptance, and the grey lines the trajectories outside the acceptance. The static bucket is indicated with the red line. The small closed circle (blue) corresponds to an unstable fixed point.

are fixed. The trajectory in the longitudinal phase space is still unique when the synchronous phase and bucket height are fixed while the synchrotron tune can then be a free parameter. Figure 1 shows longitudinal phase space topologies including the energy-dependent synchrotron radiation loss for the synchronous phase of 2.71 rad (155 deg) and the static bucket height of 5% according to Eq. (7).

One sees in Fig. 1 that the acceptance phase-space plot has the shape of a "golf club" with its "shaft" extending toward the neighboring bucket. It is well known that such a golf-club shape appears when the rf acceleration is taken into account (see, e.g., [9]). It, however, originates from the energy-dependent synchrotron radiation loss and the energy recovery from the rf field in electron storage rings.

The particles not only in the static bucket but also in the shaft can finally be trapped. When the height and width of the tilted shaft are sufficient for the energy and time spread of the bunch generated by an injector, one can inject a bunch at a point equidistant to two successive circulating bunches at the expense of a slightly higher energy from the injector. The injected bunch will be merged to the circulating bunch thanks to the longitudinal synchrotron radiation damping.

Since the injected bunch can be longitudinally separate from the circulating bunches, a transverse on-axis injection is realized with a pulsed dipole kicker, as in the common procedure for fast injection. When the pulse length of the kicker is shorter than the bunch spacing (taking the bunch length into account), the kicker field is fully transparent to the circulating bunches. Therefore, such an injection scheme fulfills our goals.

Figure 2 shows the layout of the injection devices for the conventional scheme and the longitudinal injection scheme together with beam orbits. In the latter, the injection orbit needs to be matched to the off-momentum closed orbit corresponding to the higher injection energy.

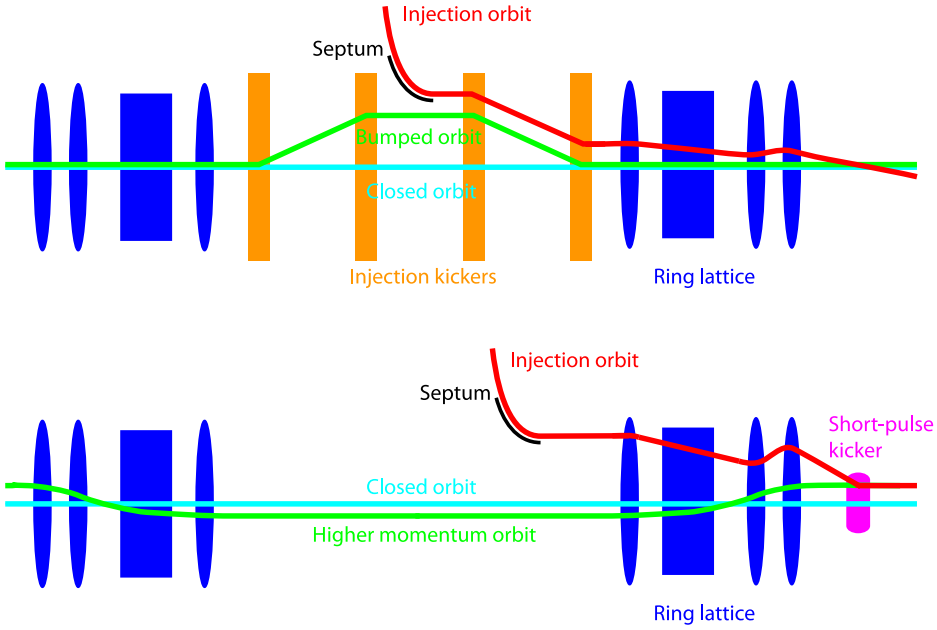

FIG. 2. Schematic layout of injection devices for the conventional scheme (top) and the longitudinal injection scheme (bottom). Injection and circulating beam orbits are also indicated.

TABLE I. Parameters relevant to the longitudinal injection. Values are from our ELEGANT simulation [12].

Parameter	Value
Circumference	528 m
Beam energy	3 GeV
Momentum compaction	3.07×10^{-4}
Damping partition $H/V/L$	1.53/1.0/1.47
Radiation loss per turn	0.58 MeV
RF frequency	100 MHz
RF voltage	1.42 MV
Third harmonic voltage	0.42 MV
Hor. equilibrium emittance	0.25 nm
Damping time, $H/V/L$	11.8/18.1/12.3 ms
Betatron tune, H/V	42.20/16.28

III. APPLICATION TO MAX IV LATTICE

We present an application of the longitudinal injection scheme to the lattice of the MAX IV 3 GeV storage ring [10] with numerical simulations. We used the ELEGANT code [11] and a lattice with two damping wigglers [12]. The aim of this simulation study is to show the feasibility of the longitudinal injection scheme. Hence the parameters and configurations presented may not be fully consistent with the actual MAX IV storage ring.

The rf voltage is determined to realize a bucket height of about 5% including a third harmonic cavity for bunch prolongation. The relevant parameters are listed in Table I, and the lattice functions are shown in Fig. 3.

We assume that the normalized rms transverse emittance of the injection beam is 10 μm (corresponding to a geometrical emittance of 1.7 nm at 3 GeV) in both planes, a relative energy spread of 0.1% and a bunch length of 5 ps. These values are taken from Ref. [13]. The bunch described above is injected with a time offset of −5 ns with respect to a circulating bunch, which corresponds to exactly the point equidistant to two successive circulating bunches, and a relative energy offset of +4.3%.

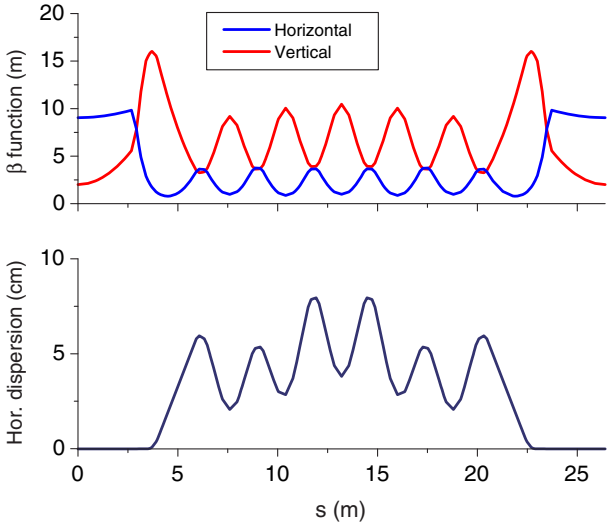

FIG. 3. Lattice functions of the seven-bend-achromat cell of MAX IV 3 GeV storage ring. The ring is composed of 20 cells.

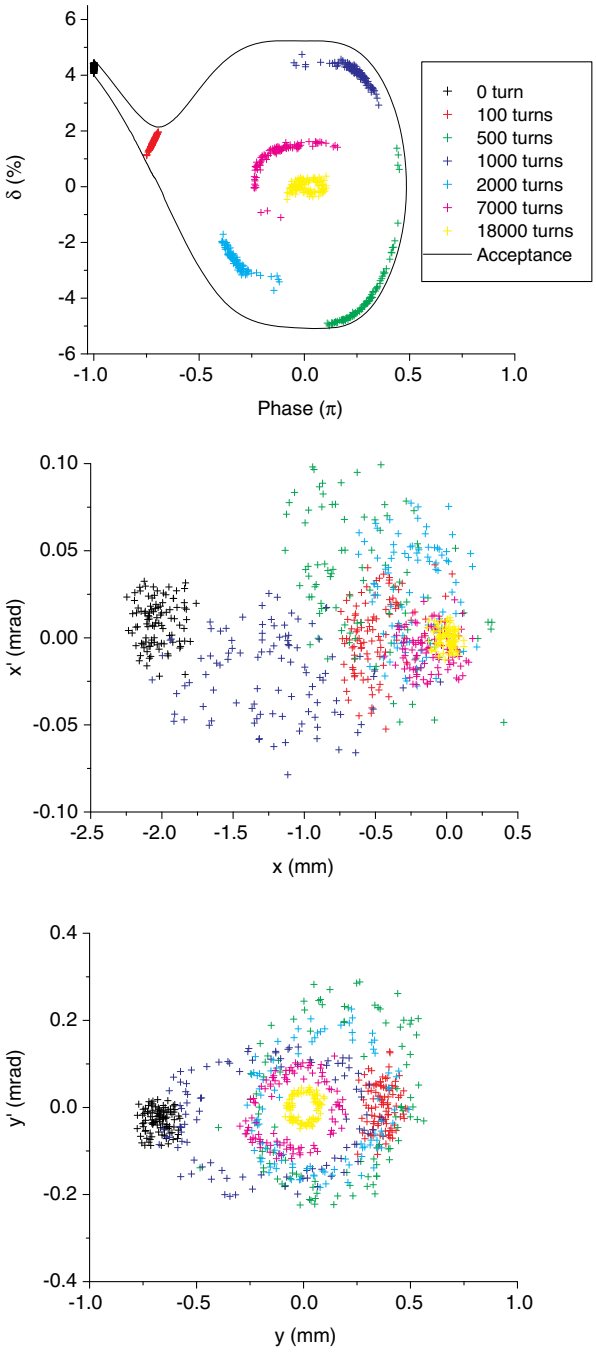

FIG. 4. Particle distributions in the longitudinal (top) and transverse (center and bottom) planes with up to 18000 turns following the injection (corresponding to 2.68 times of the damping time in the horizontal plane, 1.75 times in the vertical plane, and 2.58 times in the longitudinal plane). The closed orbit for the off-momentum injected beam (4.3%) is horizontally/vertically shifted by −1.4 mm/ − 0.2 mm due to higher order dispersion terms and the introduced machine errors. The bunch is injected at $x = -1.9$ mm and $y = -0.7$ mm.

To simulate a realistic machine, the following random machine errors are introduced:

(i) vertical sextupole misalignments of 50 μm rms and quadrupole roll errors of 0.2 mrad rms, exciting linear coupling resonances,
(ii) beta-beating of 3–6% rms through quadrupole gradient errors, exciting normal resonances,
(iii) sextupole and octupole roll errors of 0.2 mrad rms, exciting skew resonances.

In addition, the bunch is injected with a transverse offset of 0.5 mm with respect to the off-momentum closed orbit in the middle of the straight section, where the horizontal and vertical beta functions are about 9 m and 2 m, respectively. This corresponds to possible injection errors.

We generated 100 machines with different random seeds and confirmed an injection efficiency of 100% for all but one, which gave an efficiency of 95%. Even for the worst case, an efficiency of 100% was achieved by decreasing the injection error from 0.5 mm to 0.2 mm. The injection error may be reduced to 0.2 mm or less, when the tuning is performed using a modern beam position monitor system capable of reading out turn-by-turn beam positions. Figure 4 shows the particle distributions in the longitudinal and transverse planes for one of the simulation results.

It is seen that the injected bunch with the energy offset and time offset is successfully trapped to the rf bucket. The transverse oscillations due to the initial injection error are also damped as the number of turns increases.

We present a fast injection orbit with two short pulse kickers in Fig. 5. An orbit separation of about 10 mm at the septum is achieved with a kick of 1.8 mrad for each kicker, allowing the use of a common magnetic septum.

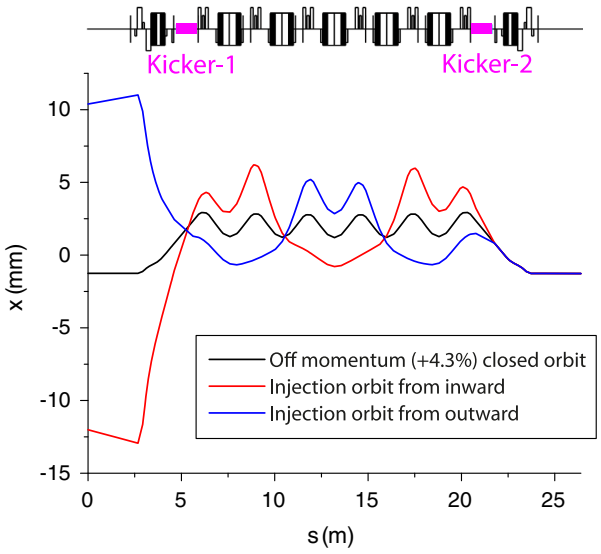

FIG. 5. Fast injection orbit with two short pulse kickers. The kick angle is 1.8 mrad for each kicker. Magenta boxes in the schematic lattice layout indicate the location of the kickers, where a straight section of about 1.3 m is available for each kicker.

TABLE II. Kicker main parameters for the application described in Sec. III. The pulse length should be slightly shorter than the rf period (10 ns for 100 MHz) because of the finite bunch length. The transverse voltage (see text) is derived from the beam energy of 3.13 GeV ($\delta = +4.3\%$) and the kick angle of 1.8 mrad.

Parameter	Value
Length	<1.3 m
Pulse length	<10 ns
Kick angle	1.8 mrad
Transverse voltage	5.63 MV

IV. SHORT PULSE KICKER

One technical challenge in the longitudinal injection scheme would be the short pulse kicker used to situate the injected bunch on-axis. We discuss in this section if the kicker required in the application described in Sec. III is feasible. The kicker main parameters are summarized in Table II.

There are a few strip-line type kickers in operation whose pulse lengths are short enough for the required pulse length of < 10 ns [14,15]. Therefore we assume here the same technology for our kicker. The strip-line type kicker in general (see, e.g., [16]) consists of a vacuum chamber that accommodates two strip-line electrodes inside. The electrodes are accessible outside the vacuum via feedthroughs at

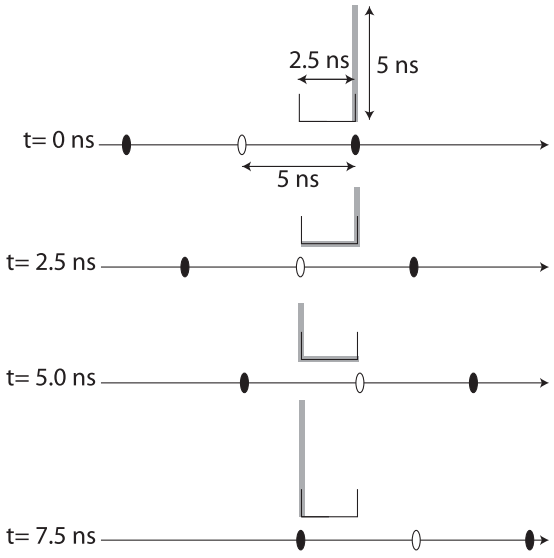

FIG. 6. Schematic time-sequence diagram of circulating and injected bunches, and kicker input pulse for a ring with 100 MHz rf system. The grey thick line represents the input pulse, propagating along the electrode. The closed ellipses represent the circulating bunches, and the open ellipse represents the injected bunch. The kicker efficiency is maximized with a length of 0.75 m (corresponding to a transit time of 2.5 ns, a quarter of the bunch spacing), i.e., the kicker can be fully filled with the input pulse during the transit of the injected bunch without deflecting the circulating bunches.

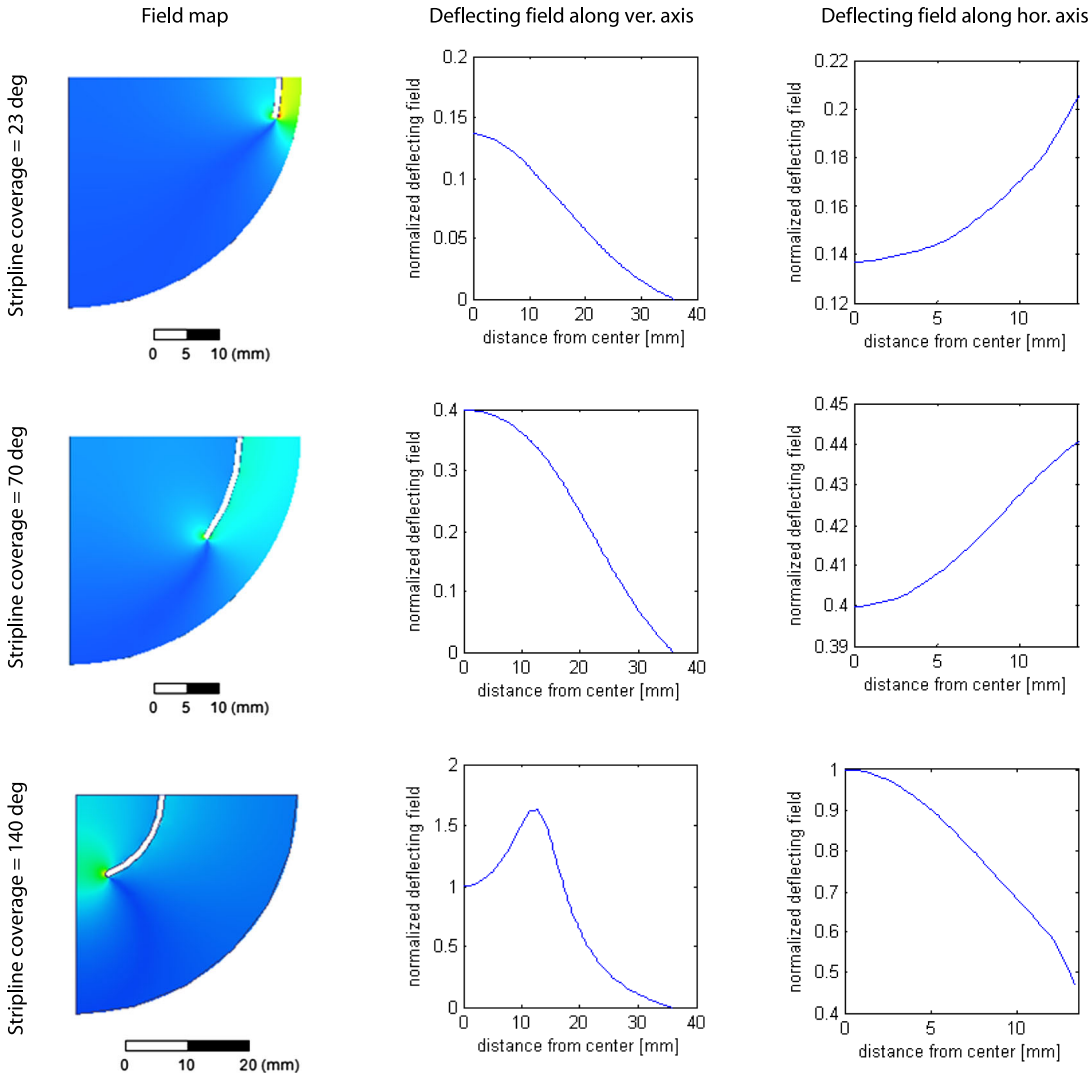

FIG. 7. Deflecting field map and profile of strip-line pulse kicker for various coverage angle. The deflecting field profiles are normalized to the on-axis field of 140 degree coverage angle.

both ends. A pulse generator is connected to one end of each strip-line, while the other end is terminated by a load matched to the strip-line differential mode characteristic impedance. The input pulses are fed with equal amplitudes but opposite polarities from the downstream ends of the kicker with respect to the beam direction such that the electric and magnetic fields both contribute to the beam deflection rather than canceling each other (the net contribution is referred to as the transverse voltage).

The maximum kicker efficiency is obtained when the kicker length is a quarter of the circulating bunch spacing and the input pulse length is half (see Fig. 6).

We performed field computations using the HFSS code [17] to estimate the impedance of various strip-line geometries. Figure 7 shows the field map and the field profile for simple round cross sections (see Fig. 8). Various strip-line coverage angles are examined for a fixed electrode voltage (pulser voltage). The characteristic impedance is adjusted to a common termination resistance of 50 Ω for all geometries. The field profiles are normalized to the value computed at the kicker center for the largest coverage angle. It is shown that the largest coverage angle provides

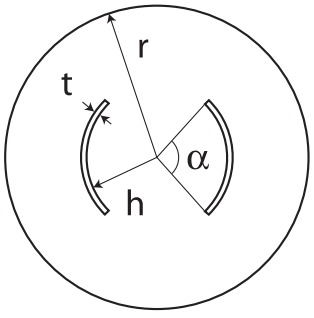

FIG. 8. Strip-line cross section in field computation. α is the coverage angle, h is the strip-line aperture radius, t is the strip-line thickness, and r is the outer vacuum chamber radius.

TABLE III. Kicker specifications based on field computation. In cases, where the tapering is applied, the coverage angle varies from 120 to 20 degrees over 50 mm. α is the strip line coverage angle, T_p is the input pulse duration, R is the strip-line shunt impedance, V_r is the required pulser voltage for an ideal rectangular input pulse shape, V_t for a trapezoidal shape with rise/fall time of 0.5/2.0 ns, and N_p is the total number of pulsers required. The following parameters are constant for all cases: the aperture radius is 11 mm, the strip-line thickness is 1.5 mm, and the outer vacuum vessel radius of 23.2 mm. The characteristic impedance is matched to 50 Ω in all cases.

Length (m)	Tapering	α (deg)	T_p (ns)	R (kΩ)	V_r (kV)	V_t (kV)	N_p
0.75	No	120	5.0	695	33.8	45.2	4
0.75	Yes	120–20	5.0	610	36.1	45.6	4
0.5	No	120	6.6	309	25.3	25.5	8
0.5	Yes	120–20	6.6	252	28.1	28.2	8

the highest deflecting field at the kicker center. The coverage angle is, however, limited by the good-field region required. In our case, due to the small beam transverse size, a large good-field region is not required, and thus a large coverage angle can be employed. Another limitation is the outer vacuum chamber radius, which becomes larger as the coverage angle increases to maintain the characteristic impedance of 50 Ω. We select a coverage angle of 120 degrees.

The transverse voltage of 5.63 MV is achieved with a 0.75 m long kicker with a strip-line aperture radius of 11 mm, a coverage angle of 120 degrees, and an electrode voltage of ±33.8 kV. The aperture radius of 11 mm corresponds to the vacuum chamber aperture of the MAX IV ring.

The pulser voltage of 33.8 kV is for an ideal rectangular input pulse shape. However, the rise and fall times due to the pulser switching are finite (trapezoidal pulse). The measured values in Ref. [15] are 0.5 ns and 2 ns, respectively. These values result in a smaller deflecting angle for the 0.75 m long kicker (−25%) than with an ideal rectangular input pulse. In other words, a higher pulser voltage (45.2 kV) is required to achieve the required kick angle. The coverage angle may be varied along the kicker (tapering) to minimize the kicker beam impedance and the reflections at the pulse generator input ports [15]. This also increases the required pulser voltage because of the reduced strip-line impedance.

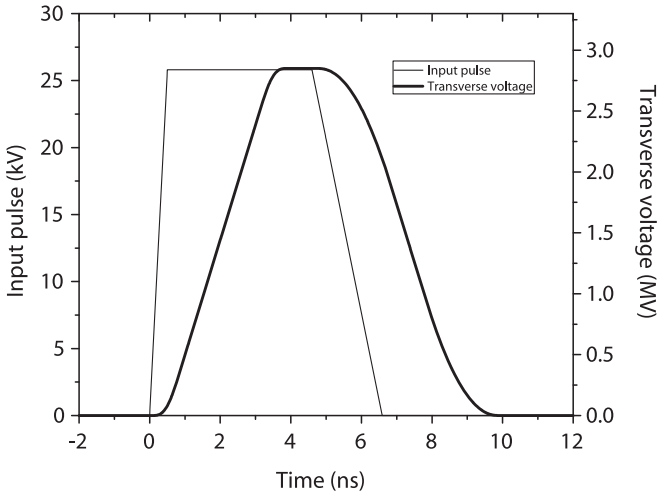

FIG. 9. Transverse voltage and input pulse for the 0.5 m long kicker with tapering (the last row of Table III).

In order to lower the pulser voltage, the kicker can be divided into two short ones. A set of two 0.5 m long kickers may comfortably fit to the straight section of 1.3 m. It is noted that this configuration requires eight pulsers in total in the MAX IV application. Table III summarizes the specifications of the kicker for the above-described cases.

The transverse voltage as a function of time for the 0.5 m long kicker with tapering is shown in Fig. 9 together with a trapezoidal input pulse.

Since our pulser specifications are similar to the ones in Ref. [15] in terms of both pulse duration and voltage, we conclude that the kicker required for the MAX IV application is feasible.

V. DISCUSSION

We find from the simulations for the MAX IV 3 GeV storage ring that the injection scheme is robust against realistic machine errors. This is consistent with the fact that the multipole magnets are properly installed and tuned in the lattice to ensure the (off-momentum) dynamic aperture [18]. The light source storage rings should be capable of accepting Touschek scattered particles so as to realize a sufficient beam lifetime. The dynamic aperture necessary for the longitudinal injection is thus a prerequisite of the storage ring for user operation. When the machine includes rather large errors at the early stage of the commissioning and the dynamic aperture is not sufficient for the longitudinal injection, one may inject bunches into the center of the rf buckets and on-axis transversely with the very same injection devices. Beam-based alignments and optics corrections may then be applied with low-current beams (i.e., without accumulation) until the dynamic aperture is sufficiently recovered.

The 100 MHz rf frequency of the MAX IV 3 GeV ring was selected, taking into account higher order mode issues, initial cost, ease of operation, etc. [10] while most light

sources are equipped with a 500 MHz rf system. A drawback due to the lower frequency is the deterioration in time resolution for time-resolved experiments because of the longer bunch length [19]. In the future, some of these experiments may move to FEL facilities, but others may stay at third generation light sources. The proposed injection scheme is presently available only for rings with low frequency rf. Research and development of "nanosecond kickers," i.e., with a pulse length of about 1 ns, is necessary to adapt the injection scheme to storage rings with a common 500 MHz rf system. Although the rise time of a pulser with MOSFET (metal-oxide-semiconductor field-effect transistor) switch is limited to a few ns [20] with present technology, a pulser with FID (fast ionization dynistors) switch [21] may fit our purpose. A pulser capable of generating such short pulses is now commercially available [22], and a nanosecond kicker may be technically feasible. The kicker needs to be divided into short segments (≤ 0.15 m), taking into account the transit time of the electron bunch and the input pulse.

With respect to the longitudinal acceptance, the "shaft" phase space must be of sufficient height and width relative to the energy spread and the bunch length of the injection bunch. The energy and phase acceptances are computed through numerical integration of Eqs. (1) and (2), and shown in Fig. 10.

The phase acceptance of 0.1 rad corresponds to 32 ps ($\sim$160 ps) for an rf frequency of 500 MHz (100 MHz). Therefore, the energy and phase acceptance would be sufficient when the bucket height is $\sim$3% (corresponding to $>$0.2% energy acceptance), at least for a linac injector. The jitter tolerances on the injection beam energy and timing are then $\ll$0.2% and $\ll$32 ps ($\ll$160 ps), respectively. Typical energy and timing jitter specifications for FEL linacs are 0.1% and 100 fs, respectively, and these values are achieved (e.g., 0.02% rms energy stability [23]). The beam jitters for ring injection can be much smaller because the bunches can be accelerated at on-crest phase with no bunch compression. Therefore, the beam jitter may not be an issue for linac injectors. A higher bucket height may allow one to employ a booster synchrotron as an injector, which in general generates injection bunches with larger energy spread and longer bunch length compared to a linac injector.

It is noted that the acceptance decreases when the damping partitions are shifted by means of combined function dipole magnets, and the longitudinal damping consequently weakens. The manipulation of damping partition is effective in lowering the natural horizontal emittance. It is also employed by the MAX IV lattice used here. The Elegant simulations presented in Sec. III likewise include this effect.

The orientation of the shaft may depend on the voltage of the third harmonic cavity. When it is a passive cavity, the voltage increases with increased stored beam current.

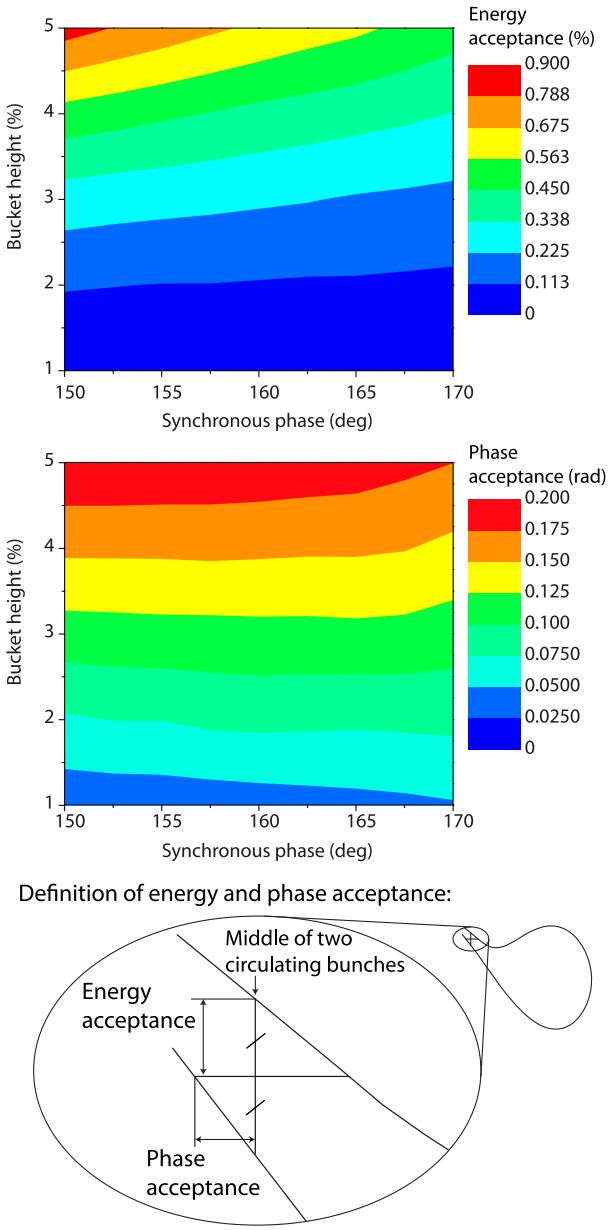

FIG. 10. Energy (top plot) and phase (center plot) acceptance. They are defined as shown schematically at the bottom.

Figure 11 depicts the longitudinal acceptance with and without the third harmonic cavity for the parameters of Table I. It is computed through tracking with Elegant and thus the reduction of the longitudinal damping partition is taken into account.

For the parameters of Table I, the shafts with and without third harmonic cavity are not overlapping. The mean energy of the injection bunch then needs to be slightly varied during the accumulation. The injection beam line magnets, the injection septum magnet and the short pulse kicker(s) all have to be adjusted with the change in beam energy. These adjustments impose an additional complexity to the operation. This is not, however, a fundamental issue.

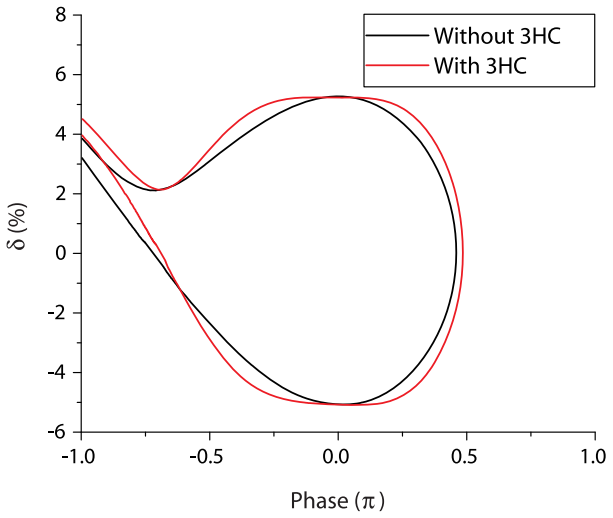

FIG. 11. Acceptance with and without third harmonic cavity. See Table I for the relevant parameters.

The requirement on the ripple of the kicker is rather loose. A possible ripple of the kicker amplitude results in an injection error, i.e., how far off-axis the injection bunch is injected. A ripple of 1% results in an injection error of about 100 μm since the orbit separation at the septum is about 10 mm. According to the tracking study in Sec. III an injection error of 100 μm does not deteriorate the injection efficiency. Therefore a ripple of 1% (or higher) can be tolerated.

So far, only the longitudinal injection scheme and the swap-out injection scheme fulfil our goals, and their advantages and disadvantages are considered in the following. One disadvantage in the swap-out injection is that a full charge injector is required. The dead-band in bunch-by-bunch swapping would be larger than that of the conventional top-up injection since it may not be straightforward to generate full charge injection bunches with bunch charge fluctuation on the order of 10^{-3}. Furthermore, the amount of dumped beam in a bunch-by-bunch swapping is several orders of magnitude higher than that of the conventional top-up injection. Although it can be localized, it may not be trivial in practice to include a dedicated shielding to the facility. The bunch train swapping requires another ring to store the beam and keep it ready for swapping. Therefore, the initial construction cost of the facility is much higher and the electricity consumption during operation is significantly increased. The longitudinal injection scheme is not applicable to the low-alpha operation mode [24], in which the longitudinal acceptance is not suitable. Concerning the dipole kicker, it is noted that the pulse length in a bunch-by-bunch swap-out injection can be about twice as long as the one required for the longitudinal injection. In a bunch train swapping, a long pulse kicker with a stable flat-top is required, and the injection error is a potential issue for the photon beam stability.

VI. CONCLUSION

We have presented a new on-axis top-up injection scheme for small aperture electron storage rings. It is shown that the longitudinal acceptance phase-space plot has the shape of a golf club similar to the longitudinal motion with rf acceleration. However, it originates not from acceleration but from the energy-dependent synchrotron radiation loss present in electron storage rings. The shaft of the golf club extending to the neighboring bunch allows one to inject a bunch at a point equidistant to two successive circulating bunches. The temporal separation enables the use of dipole kickers, and the injected bunch can be situated transversely on-axis. The injection process is fully transparent to the circulating bunches, ensuring photon beam stability. An application to the lattice of the MAX IV 3 GeV storage ring revealed the feasibility and robustness of the injection scheme.

For a lower frequency rf (∼100 MHz as in the MAX IV example), the required short pulse kicker (∼10 ns) is available with present technology. A very short pulse kicker (∼1 ns), which is technically feasible, allows us to apply the injection scheme to storage rings with a common 500 MHz rf system.

ACKNOWLEDGMENTS

We would like to thank M. Carlà, J. Chrin, T. Garvey, S. C. Leemann, L. Rivkin, and T. Schietinger for fruitful discussions.

[1] S. Nakamura *et al.*, Present status of the 1 GeV synchrotron radiation source at sortec, in *Proceedings of European Particle Accelerator Conference, Nice, France, 1990*, (Editions Frontiéres, Gif-sur-Yvette, 1990), p. 472.

[2] H. Ohkuma, Top-up operation in light sources, in *Proceedings of the 11th European Particle Accelerator Conference, Genoa, 2008* (EPS-AG, Genoa, Italy, 2008), p. 36.

[3] C. Gough and M. Mailand, Septum and kicker systems for the SLS, in *Proceedings of the Particle Accelerator Conference, Chicago, IL, 2001* (IEEE, New York, 2001), p. 3741.

[4] H. Takaki, N. Nakamura, Y. Kobayashi, K. Harada, T. Miyajima, A. Ueda, S. Nagahashi, M. Shimada, T. Obina, and T. Honda, Beam injection with a pulsed sextupole magnet in an electron storage ring, Phys. Rev. ST Accel. Beams **13**, 020705 (2010).

[5] L. Emery and M. Borland, Possible long-term improvements to the advanced photon source, in *Proceedings of the 2003 Particle Accelerator Conference, Portland, OR* (IEEE, New York, 2003), p. 256.

[6] P. Collier, Synchrotron phase space injection into LEP, in *Proceedings of the Particle Accelerator Conference, Dallas, TX, 1995* (IEEE, New York, 1995) p. 551.

[7] E. Levichev (private communication).

[8] K. Wille, *The physics of particle accelerators* (Oxford University Press, New York, 2000) ISBN 0-19-850549-3 (2000).
[9] P. M. Lapostolle, Proton linear accelerators: A theoretical and historical introduction, Los Alamos National Laboratory Report No. LA-11601-MS, 1989.
[10] "MAX IV Detailed Design Report", https://www.maxlab.lu.se/maxlab/max4/index.html.
[11] M. Borland, Elegant: A flexible SDDS-compliant code for accelerator simulation, Advanced Photon Source Report No. LS-287, 2000.
[12] A Tracy-3 lattice file (courtesy of S. C. Leemann) is converted to an Elegant lattice file.
[13] S. C. Leemann, Pulsed sextupole injection for Sweden's new light source MAX IV, Phys. Rev. ST Accel. Beams **15**, 050705 (2012).
[14] T. Naito, H. Hayano, M. Kuriki, N. Terunuma, and J. Urakawa, Development of a 3 ns rise and fall time strip-line kicker for the international linear collider, Nucl. Instrum. Methods Phys. Res., Sect. A **571**, 599 (2007).
[15] D. Alesini, S. Guiducci, F. Marcellini, and P. Raimondi, Design, test, and operation of new tapered stripline injection kickers for the e^+ e^- collider $DA\Phi NE$, Phys. Rev. ST Accel. Beams **13**, 111002 (2010).
[16] D. A. Goldberg and G. R. Lambertson, Dynamic Devices A Primer on Pickups and Kickers, Lawrence Berkeley Laboratory Report No. LBL-31664 ESG-160, 1992.
[17] ANSYS HFSS from ANSYS Inc., Southpointe, 275 Technology Drive, Canonsburg, PA 15317, USA.
[18] S. C. Leemann, Å. Andersson, M. Eriksson, L.-J. Lindgren, E. Wallén, J. Bengtsson, and A. Streun, Beam dynamics and expected performance of Sweden's new storage-ring light source: MAX IV, Phys. Rev. ST Accel. Beams **12**, 120701 (2009).
[19] MAX IV includes the Short Pulse Facility, which utilizes the injector linac and generates FEL radiation, to provide users with beamlines for time-resolved experiments at the same site [10].
[20] M. J. Barnes, T. Fowler, G. Ravida, and A. Ueda, Design of the modulator for the CTF3 tail clipper kicker, in *Proceedings of the 22nd Particle Accelerator Conference, PAC-2007, Albuquerque, NM* (IEEE, New York, 2007), p. 2185.
[21] V. M. Efanov, V. V. Karavaev, A. F. Kardo-Sysoev, and I. G. Tchashinikov, Fast ionization dynistor (FID)-a new semiconductor superpower closing switch, in *Proceedings of Pulsed Power Conference, Baltimore, MA, USA, 1997*, (IEEE, Piscataway, 1997), p. 988.
[22] http://www.fidtechnology.com/.
[23] T. Asaka, T. Hasegawa, T. Inagaki, H. Maesaka, T. Ohshima, S. Takahashi, K. Togawa, and Y. Otake, Stability performance of the injector for SACLA/XFEL at SPring-8, in *Proceedings of the 26th Linear Accelerator Conference, Tel Aviv, Israel* (JACoW, Tel Aviv, 2012), p. 486.
[24] C. Pellegrini and D. Robin, Electron density enhancement in a Quasi isochronous storage ring, in *Proceedings of the 1991 Particle Accelerator Conference, San Francisco, CA, 1991* (IEEE, New York, 1991), p. 398.